Absolute emission cross sections for electron-impact excitation of $Zn^+(4p\ ^2P)$ and $(5s\ ^2S)$ terms. I

Wade T. Rogers,* Gordon H. Dunn,† J. Østgaard Olsen, Melissa Reading, and G. Stefani‡
Joint Institute for Laboratory Astrophysics,
University of Colorado and National Bureau of Standards, Boulder, Colorado 80309
(Received 26 May 1981)

Absolute emission cross sections for electron-impact excitation of the $3d^{10}4p\ ^2P$ and $3d^{10}5s\ ^2S$ terms of Zn^+ have been measured from below threshold to about 790 eV (^2P) and 388 eV (^2S) using the crossed-charged-beams technique. Both transitions have the abrupt onset at threshold characteristic of positive-ion excitation. The ^2P cross section shows considerable structure in the interval from threshold to near 20 eV, above which it falls off smoothly. Agreement with five-state close-coupling theory is excellent below 100 eV when cascading is included in the theory. Above 100 eV, the data lie above the theory. The peak value of the ^2P cross section is 9.4×10^{-16} cm^2 essentially at threshold, while the peak value of the ^2S cross section is about 0.47×10^{-16} cm^2. The net linear polarization of the $3d^{10}4p\ ^2P$ emission was measured (unresolved from the $3d^{10}4d\ ^2D\rightarrow3d^{10}4p\ ^2P$ cascading transition), and these data were used to correct the cross-section data for anisotropy of the emitted light. The *effective* lifetime of the $3d^9 4s^2\ ^2D_{3/2}$ level was measured by observing exponential decay of the 589.6-nm photons resulting from its decay.

I. INTRODUCTION

The development of magnetically confined controlled-thermonuclear-reactor (CTR) plasmas is complicated by the existence of heavy, partially stripped species which may have an important effect on energy balance. In particular, the electron-impact-excited resonance lines of partially stripped Cu-like systems have been identified[1] as being potentially important in terms of radiative energy loss in the next generation of magnetically confined plasmas. Reliable calculations of energy loss and plasma spectra await experimental checks of the collision theories used to predict cross sections, and this paper is intended to fill partially this need.

We have measured absolute total emission cross sections for the processes

$$e+Zn^+(4s\ ^2S_{1/2})\rightarrow e+Zn^+(nl\ ^2L)$$
$$\rightarrow h\nu 202.5,\ 206.2\ \text{nm}, \quad (1)$$
$$\rightarrow h\nu 250.2,\ 255.8\ \text{nm}, \quad (2)$$

with the relevant levels shown in the term diagram of Fig. 1. The process in Eq. (1) is dominated by excitation of the resonance level, $nl\ ^2L\equiv4p\ ^2P_{1/2,3/2}$, but includes cascade contributions from higher-lying levels which are dipole connected with $4p\ ^2P$. The process in Eq. (2) is dominated by excitation of the $5s\ ^2S_{1/2}$ level which decays by emission of a photon to the $4p\ ^2P$ resonance term but also includes cascade contributions from higher-

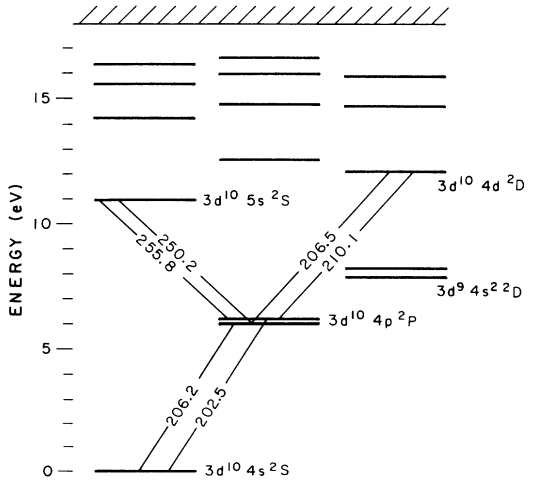

FIG. 1. Partial term-level diagram for Zn^+. Wavelengths are in nm.

lying levels. Transitions from the $5s\,^2S_{1/2}$ level also represent a single cascade contribution to Eq. (1). Cross sections were measured as a function of incident energy from below threshold to 789 eV for $4\,^2P$ excitation, and to 388 eV for $5\,^2S$ excitation. Additionally, the net polarization of the resonance multiplet was measured from 10 to 789 eV, and from these data the polarization of the $4\,^2P_{3/2}$ emission was inferred (the $4\,^2P_{1/2}$ line is theoretically unpolarized).[2] These data were also used to derive a correction due to the anisotropy of the emitted light. The polarization of the $5\,^2S_{1/2}$ emission is also expected[2] to be zero, and was not measured.

During initial measurements it was discovered that there was a large background at our Zn^+ resonance-line detector due to higher-lying metastable Zn^+ ions in the beam which decay by transitions to the $3d^{10}4p\,^2P$ term, giving rise to a resonance-line photon. In part to determine the level of metastable contamination in the target ion beam, we undertook a rather crude measurement of the lifetime of the contributing metastable level.

II. EXPERIMENTAL PROCEDURE

The experiment consists of bombarding target Zn^+ ions with variable-energy electrons and measuring a known fraction of the photons produced from the resulting excitation of the Zn^+ ions. The crossed-charged-beams apparatus used for this work is shown schematically in Fig. 2, and has been thoroughly described in the literature.[3–7] The present discussion of the apparatus includes only those aspects peculiar to this work.

A. Derivation of the cross section from measured quantities

The cross section is obtained from measured quantities from the equation

$$\sigma=\frac{1}{Y_\Omega}\frac{\mathscr{R}}{I_iI_e}\frac{e^2v_iv_e}{(v_i^2+v_e^2)^{1/2}}\frac{\mathscr{F}}{D(z_0,\lambda)}\,. \tag{3}$$

Here, σ is the emission cross section, $\mathscr{R}$ is the photon count rate, e is the electronic charge, I_i and I_e are the total currents of ions and electrons, and v_i and v_e are the respective velocities. The factor Y_Ω corrects for anisotropy of the radiation and takes into account the finite detector solid angle Ω. It is given in terms of θ, the angle between the photon trajectory and electron beam axis, by

$$Y_\Omega=(1-P\langle\cos^2\theta\rangle_\Omega)/(1-P/3)\,, \tag{4}$$

where P is the polarization of photons emitted along the detection axis, and $\langle\cos^2\theta\rangle_\Omega$ is the average value of $\cos^2\theta$ over the detector solid angle. The form factor $\mathscr{F}$ accounts for the spatial overlap of the beams and the spatial variation of detector sensitivity. Let axes x, y, and z be, respectively, the directions of ion beam, electron beam, and the axis of observation of photons. Also, let $R(z)$ and $G(z)$ represent ion- and electron-beam density distributions along the z axis and let $\eta(z,\lambda)$ represent

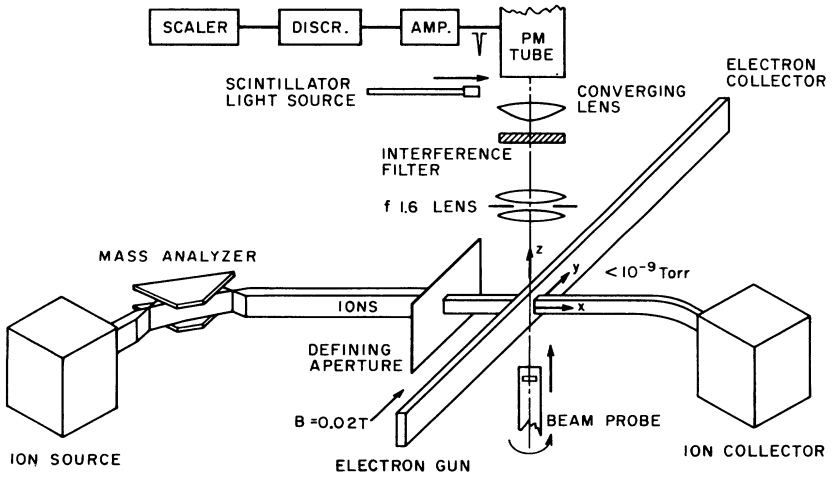

FIG. 2. Schematic of crossed-charged beams arrangement used to measure Zn^+ excitation.

the relative detector sensitivity profile. The form factor is then given by

$$\mathcal{F}=\frac{\int R(z)dz\int G(z)dz}{\int R(z)G(z)\eta(z,\lambda)dz}\ , \tag{5}$$

where

$$\eta(z,\lambda)=D_R(z,\lambda)-I_1+(e^{w_e/v_i\tau}-1)I_2\ , \tag{6}$$

with

$$I_1=\frac{\int_0^{w_e}e^{-x/v_i\tau}D_R(x,z,\lambda)dx}{\int_0^{w_e}D_R(x,z_0,\lambda)dx} \tag{7}$$

and

$$I_2=\frac{\int_{w_e}^{\infty}e^{-x/v_i\tau}D_R(x,z,\lambda)dx}{\int_0^{w_e}D_R(x,z_0,\lambda)dx}\ . \tag{8}$$

The quantity $D(z_0,\lambda)$ in Eq. (3) is the average probability that a photon emitted in an arbitrary direction from the $z=z_0$ plane in the collision volume will be counted, and $D_R(z,\lambda)$ in Eq. (6) is the relative variation of that probability with height z, normalized such that $D_R(z_0,\lambda)=1$. $D_R(x,z,\lambda)$ is the relative probability averaged over the width of the ion beam that a photon emitted from a line parallel to the electron beam will be detected, w_e is the width of the electron beam, and τ is the lifetime of the transition yielding photons of wavelength λ. In Eq. (6) the subtraction of I_1 accounts for the fact that, due to their finite lifetime, some ions do not radiate while within the electron beam, while the term including I_2 accounts for emission beyond the electron beam which is still detected.

B. Ion source

Zn^+ ions are produced in a commercial, hot cathode discharge ion source.[8] Pure Zn metal is introduced into the source in a small stainless-steel sample holder. The metal is vaporized by the hot filament and a discharge is struck in the pure Zn vapor. No support gas is required due to the relatively high vapor pressure of Zn, enabling operation of the ion source with no measurable gas load on the interaction chamber.

As previously mentioned, it was found during initial tests that the ion source produced ions in high-lying metastable levels. Though the effective lifetime of these levels[9] is short enough that the metastable contamination is negligible ($<0.5\%$) with respect to determination of ground-state target density, it is nevertheless a problem because the metastable levels decay predominantly through the resonance level, giving rise to unacceptably large photon background counting rates. However, it was possible to reduce this background to an acceptable level (lower by more than an order of magnitude) by reducing the voltage across the ion source discharge to about 12 V, which is below the 13.8-eV threshold for single-collision production of metastable ions from the Zn $3d^{10}4s^2\,{}^1S_0$ parent atoms. Operating in this mode gave a mass-analyzed Zn^+ beam of about 0.5 μA at 1000-eV beam energy with less than 0.05% metastable contamination.

C. Radiometry

The task of measuring absolute cross sections amounts to measuring all quantities in Eq. (3). This section describes techniques used to obtain the radiometric term $D(z_0,\lambda)$. Measurements of the relative detector sensitivity functions $D_R(z,\lambda)$ and $D_R(x,z,\lambda)$ were made using previously described techniques[3,4,7] and will not be elaborated upon here.

As mentioned above, $D(z_0,\lambda)$ is the average probability that a photon emitted from the $z=z_0$ plane in the collision volume will be counted. It is measured by placing a monochromatic, uniform, isotropic source of known spectral radiance at wavelength λ, whose lateral extent is equivalent to that of the collision volume, at height z_0 in the collision volume, and measuring the response of the photon detector. The spectral radiance of this "transfer light source" is in turn measured by viewing it with a vacuum photodiode whose absolute sensitivity was calibrated by the National Bureau of Standards. The transfer light source consists of a Zn discharge lamp coupled to the entrance of a 35-cm grating monochromator, a 2-mm-diameter quartz light pipe at its exit slit, and a 1-cm-diameter integrating sphere at the end of the light pipe, having a rectangular exit aperture of 2×1.5 mm^2. The intensity of the source was adjusted such that counting rates measured by the photon detection system were within its linear range (a typical calibration counting rate of 24 kHz required a 1.4% counting dead-time correction).

Prior to performing the final calibration transfer, a series of measurements was carried out to test the isotropy, monochromaticity, uniformity,

and stability of the transfer light source. Additionally, the photodiode was subjected to tests of uniformity and angle-of-incidence effects, and on the basis of these tests an optimum geometry for viewing the transfer light source with the photodiode was chosen.

The currents produced by the photodiode during the calibration were typically 5×10^{-14} A, and were measured with a vibrating reed electrometer. The electrometer was calibrated by separately measuring the value of the nominally 10^{12}-Ω feedback resistor and the voltage sensitivity of the circuitry measuring the voltage developed across the resistor. The combined uncertainty of these calibrations was 1.5%.

We may write the spectral radiance of the transfer light source, as determined by the photodiode, in terms of the following: $i_D(\lambda)$, the photocurrent in the diode at a transfer source wavelength of λ; $\epsilon_D(\lambda)$, the average diode quantum efficiency at λ; Ω_D, the solid angle subtended by the diode aperture at the transfer light source; and A_Ω^D, the average projected area of the transfer light source into Ω_D. The lamp in the transfer source is a line source with negligible continuum and no nearby strong lines, so that the transfer source is very effectively monochromatic, and scattered light at different wavelengths in the monochromator is negligible.

The absolute detection system sensitivity may now be written

$$D(z_0,\lambda)=e\epsilon_D(\lambda)\frac{A_\Omega^D\Omega}{A_\Omega^F}\frac{\Omega_D}{4\pi}\frac{C_F(z_0,\lambda)}{i_D(\lambda)}\ , \tag{9}$$

where $C_F(z_0,\lambda)$ is the count rate of the photon detection system in response to the transfer light source at height z_0 in the interaction volume and at wavelength λ, and A_Ω^F is the average projected source area into the detection system solid angle Ω_F.

Owing to the low intensity of the Zn^+ resonance lines at 202.5 and 206.2 nm from the discharge lamp, the statistical precision of the photodiode current measurements at these wavelengths was poor. The approach we adopted was to calibrate the detection system at the strong Zn 213.8-nm resonance line, then use the relative spectral function $D_R(z_0,\lambda)$ to extrapolate to the Zn^+ resonance lines. This function may be written as the product of the relative transmission of the detection system quartz optics and the interference filter, and the relative spectral quantum efficiency of the photomultiplier tube. In the wavelength range 202.5—213.8 nm, both the quartz and the photomultiplier are fairly flat, and $D_R(z_0,\lambda)$ is dominated by the interference filter transmission. The interference filter function was measured *in situ*, and the quartz and photomultiplier functions were determined from data supplied by the manufacturers.

The absolute sensitivity $D(z_0,213.8\text{ nm})$ was determined by performing six complete, independent calibration transfers. Each transfer consisted of measurement of the standard diode response to the transfer light source, then moving the transfer source to the detection system, where its response was measured, then moving back again to the standard. At both stations the background count rate (or current) was measured and subtracted. For each photomultiplier tube measurement a pulse height distribution was measured to determine the electronic pulse transmission, and appropriate counting dead-time corrections were applied (this correction never exceeded 1.6%). The average transfer ratio statistical uncertainty is determined from the scatter of the six individual transfers (1.5% standard deviation about the mean). The individual line sensitivities at 202.5 and 206.2 nm are determined using the function $D_R(z_0,\lambda)$, and are combined to give an average resonance multiplet sensitivity $D(z_0,\bar{\lambda}_{4p})$, under the assumption that the ^2P_J levels are statistically populated.[10]

The calibration of the $5s\ ^2S_{1/2}\rightarrow 4p\ ^2P_{1/2,3/2}$ multiplet wavelengths (250.2,255.8 nm) was carried out in a manner similar to that described above for the resonance doublet, except that a Hg discharge lamp was used in the transfer light source with the 253.7-nm line selected, and a different interference filter was used in the photon detection system to accept a wavelength range around the 5*s*-4*p* transition. The individual line sensitivities $D(z_0,250.2$ nm) and $D(z_0,255.8$ nm) were determined, as in the resonance-line calibrations, and combined, again assuming a statistical line ratio, to give an average multiplet sensitivity $D(z_0,\bar{\lambda}_{5s})$. The final result of the two calibrations were $D(z_0,\bar{\lambda}_{4p})=7.9\times10^{-5}$ count photon$^{-1}\pm$ 13%, and $D(z_0,\bar{\lambda}_{5s})=1.5\times10^{-4}$ count photon$^{-1}\pm$16%. Uncertainties quoted here are a combination of statistical and systematic uncertainties evaluated at a level judged comparable to the statistical 68% confidence level (see below), and Table I lists individual sources of uncertainty and their values for both calibrations. It is noted from Table I that at both wavelengths the total calibration uncertainty is dominated by the uncertainty in the sensitivity of the NBS-calibrated photodiode.

TABLE I. Absolute calibration uncertainties for Zn II excitation experiments.

Source of uncertainty	68% Confidence level uncertainties[a] percent 202.5, 206.2 nm	250.2, 255.8 nm
Uncertainty in NBS-calibrated photodiode	12.0	15.0
Transfer statistics	1.5	5.0
Projected source area A_Ω	0.8	0.8
Photodiode current measurement	1.5	1.5
Pulse transmission	1.0	1.0
Counting dead time	0.5	1.0
Wavelength extrapolation	2.0	1.0
Transfer light source Isotropy	1.6	1.0
Photodiode uniformity with respect to position and angle of incidence	2.0	2.0
Quadrature sum	13	16

[a]An effort was made to evaluate systematic errors at a level judged to be consistent with the statistical 68% CL.

D. Data accumulation and reduction

Measurements of the beam currents and photon counting signals required in Eq. (3) were typically made in a series of 100-sec integrations under computer control. Photon counting rates encountered in the experiment range from 2 to 8 counts sec^{-1} for signal photons and from 25 to 112 counts sec^{-1} for background events, and a beam-modulation technique was used to separate signal from background.[6,11]

Data reduction was carried out in a straightforward way using Eqs. (3)–(8). It is noted that the terms in Eq. (6) accounting for the finite lifetime of the excited state are negligibly small due to the very small product of $v_i\tau$ compared with the measured field of view of the detector. Form factors for each data point were determined to better than 1% from measured electron- and ion-beam profiles using Eq. (5),

Two other aspects of the data reduction should be pointed out. First, the distinction is made between line-emission cross sections and level-excitation cross sections. The line-emission cross section for a particular optical transition is the direct excitation cross section for the upper level involved in that transition, modified by a term accounting for the branching ratio for the observed transition and by terms accounting for cascade into the upper level. We report here line-emission cross sections, and care should be taken when making comparisons with theoretical calculations. We note in passing that there is theoretical evidence[12] that in the case of the Zn^+ resonance-line-emission cross section there is a substantial (up to a factor of 1.64) cascade contribution at some energies (see discussion below).

Second, the anisotropy correction factor Y_Ω in Eqs. (3) and (4) is derived from our measurements

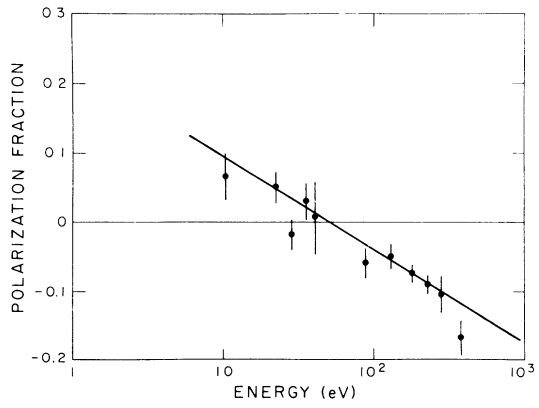

FIG. 3. Measured polarization fraction of the radiation (202.5 nm, 206.2 nm) from the $4p\ ^2P_{1/2,3/2}$ levels of Zn^+ vs impacting electron energy. (Significant cascading radiation from $4d\ ^{2D}$ at 207 and 210 nm is also included.) Line is simply a least-squares fit to the data.

TABLE II. Relative uncertainties in Zn^+ excitation experiments.

Source of uncertainty	68% Confidence level uncertainties[a] percent 202.5, 206.2 nm	250.2, 255.8 nm
Counting statistics	3.0 typical	10.0 typical
Form factor	0.5	0.5
Path length	0.5	0.5
Uncollected electrons	$+0$ $-x^b$	$+0$ $-x^b$
Electron current measurement	0.5	0.5
Ion current measurement	0.5	0.5
Pulse transmission	0.5	0.5
Quadrature sum	$+3.2$ $-(x+3.2)$	$+10.2$ $-(x+10.2)$

[a]An effort was made to evaluate systematic uncertainties at a level judged consistent with the statistical 68% CL.
[b]The one-sided uncertainty x increased with energy, ranging from about 1% at 100 eV to 14% at 800 eV. It is added linearly to the quadrature combination of the uncertainties.

of the polarization of the line radiation. In the case of the Zn^+ resonance lines the net linear polarization of the two lines was measured, weighted by the relative spectral sensitivity of the detection system. From this measurement the linear polarization of the $^4P_{3/2}$ may be deduced, assuming that the $^4P_{1/2}$ line is unpolarized[2,3,13] and that the two lines are populated according to their statistical

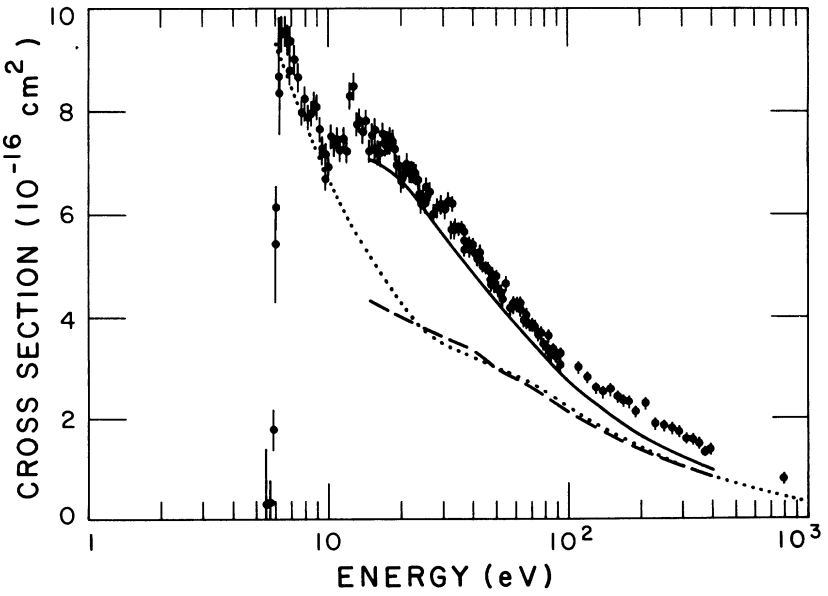

FIG. 4. Absolute line-emission cross section for 202.5 and 206.2 nm [Eq. (1)]. Present experimental results, ●; 5CC results (Ref. 12) including cascade (see text),—; 5CC results (Ref. 12) without cascade — — —; $\bar{g}$-formula results, not including cascade · · · · . Flags show representative 68% CL relative uncertainties only (Table I). Asymmetric flags at energies greater than 100 eV reflect possible effects due to uncollected electrons.

TABLE III. Absolute emission cross sections for the process of Eq. (1): $e+Zn^+(4s\ ^2S_{1/2})\rightarrow e+Zn^+(nl\ ^2L)\rightarrow h\nu(202.5, 206.2\ \text{nm})$. Numbers in parentheses[a] represent percentage total *relative* uncertainty at 68% CL. Absolute uncertainties are given in Table II.

E (eV)	σ (10^{-16} cm^2)	E (eV)	σ (10^{-16} cm^2)	E (eV)	σ (10^{-16} cm^2)	E (eV)	σ (10^{-16} cm^2)
6.25	8.39(4)	16.06	7.20(2)	32.89	6.20(2)	72.64	3.79(2)
6.41	9.59(4)	16.45	7.19(2)	33.53	5.68(3)	74.75	3.63(3)
6.65	9.56(4)	16.86	7.56(3)	33.84	5.77(2)	76.67	3.67(3)
6.80	9.38(3)	17.25	7.34(3)	34.92	5.71(2)	78.69	3.46(3)
6.94	9.08(2)	17.68	7.38(3)	35.89	5.73(2)	80.67	3.39(3)
7.24	9.01(3)	18.10	7.43(2)	36.74	5.44(2)	82.65	3.47(2)
7.49	8.66(3)	18.52	7.42(3)	37.87	5.40(2)	84.59	3.23(3)
7.77	7.98(3)	18.94	7.26(3)	38.74	5.36(2)	86.64	3.35(3)
8.01	8.24(3)	19.33	6.96(3)	38.95	5.30(2)	88.59	3.21(3)
8.24	7.88(3)	19.72	6.93(3)	39.93	5.39(2)	90.53	3.26(3)
8.48	7.95(3)	20.15	6.63(3)	40.90	5.23(2)	92.48	3.18(2)
8.74	8.14(3)	20.59	6.70(3)	41.87	5.09(2)	111	3.01(3,4)
8.95	8.08(3)	20.99	6.78(3)	42.92	5.16(2)	120	2.82(3,4)
9.24	7.65(3)	21.41	6.97(3)	43.96	4.96(2)	130	2.61(3,4)
9.47	7.24(2)	21.83	6.81(3)	44.91	4.96(2)	140	2.53(3,5)
9.73	6.92(2)	22.22	6.81(3)	45.90	4.94(2)	150	2.59(3,5)
10.00	6.91(3)	22.69	6.81(3)	46.86	4.70(2)	160	2.43(3,5)
10.28	7.51(3)	23.10	6.76(3)	47.90	4.70(2)	170	2.34(3,5)
10.59	7.35(3)	23.52	6.67(3)	48.90	4.68(2)	180	2.33(3,5)
10.90	7.45(3)	23.92	6.39(3)	50.05	4.74(2)	191	2.12(3,5)
11.18	7.24(3)	24.30	6.20(3)	50.86	4.54(3)	211	2.30(3,6)
11.58	7.46(3)	24.71	6.27(3)	51.91	4.48(3)	230	1.89(3,6)
11.92	7.22(3)	25.19	6.20(3)	52.80	4.33(2)	250	1.84(3,6)
12.31	8.30(3)	25.59	6.53(3)	54.82	4.64(3)	271	1.79(3,7)
12.74	8.49(3)	25.96	6.33(3)	56.89	4.16(3)	291	1.73(3,7)
13.15	7.75(3)	26.37	6.43(3)	58.77	4.22(2)	311	1.57(3,7)
13.53	7.82(3)	27.45	6.01(3)	60.85	4.24(3)	331	1.57(3,8)
13.97	7.60(3)	28.45	6.12(3)	62.75	4.20(2)	352	1.48(3,8)
14.37	7.81(3)	29.52	6.18(3)	64.83	3.92(3)	372	1.31(3,8)
14.80	7.22(3)	30.52	6.08(3)	66.72	3.96(2)	391	1.32(1,7)
15.20	7.53(3)	31.51	6.24(3)	68.72	3.83(3)	792	0.78(1,15)
15.63	7.46(2)	32.52	5.69(3)	70.74	3.83(3)		

[a]Single numbers in parentheses indicate a uniform uncertainty, i.e., $(x)\equiv\pm x\%$. Two numbers in parentheses indicate the inclusion of one-sided uncertainties (see text), i.e., $(x,y)\equiv+x\%-y\%$.

weights.[10] The anisotropy of the multiplet is then related in a straightforward way to the anisotropy of the $^4P_{3/2}$ line. The measured net linear polarization $\bar{P}$ of the multiplet is shown in Fig. 3 along with a least-squares fit of a straight line to the measured data used to obtain the anisotropy correction as a function of energy. The theoretical polarization of the $5\ ^2S_{1/2}-4\ ^2P_j$ multiplet is zero,[2] hence the radiation from $5\ ^2S_{1/2}$ is taken to be isotropic (i.e., $Y_\Omega\equiv 1$), and no measurement of this polarization was made.

E. Uncertainties

All statistical uncertainties are quoted at the 68% confidence level (CL), corresponding to one standard deviation of the mean. Where systematic

uncertainties occur, an effort has been made to evaluate them at a confidence level consistent with the statistical 68% CL. Where different uncertainties are judged to be uncorrelated they are combined in quadrature to give a total uncertainty. Tables I and II give breakdowns of the sources of relative and absolute uncertainties and their magnitudes.

The uncertainty in Table II due to uncollected electrons has been discussed previously.[3,4] It is largely due to low-energy secondary electrons produced on surfaces by beam electrons backscattered from the electron-beam collector. This uncertainty is one-sided (the cross section may be lower than reported) and an increasing function of energy above 100 eV; below 100 eV it is essentially negligible. In Figs. 4 and 6 a few representative one-sided error flags are included above 100 eV to indicate the uncertainty from this source.

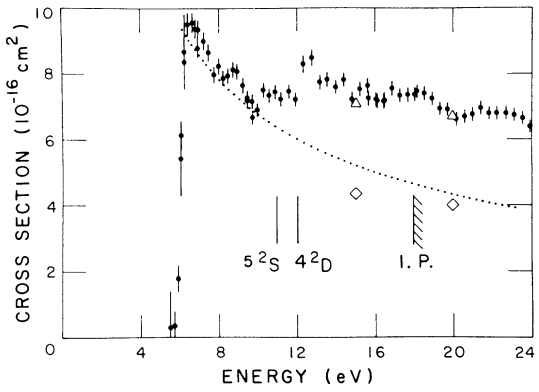

FIG. 5. Near-threshold resonance-line-emission cross section [Eq. (1)]. Present measurements, ●; 5CC calculations (Ref. 12) including cascade, △ ; 5CC calculations (Ref. 12) without cascade, ◇; $\bar{g}$ predictor formula, no cascade, dotted curve. Flags represent relative 68% CL uncertainties as in Fig. 4. Thresholds for major cascading states are indicated.

III. RESULTS AND DISCUSSION

A. Resonance-line-emission cross sections

The results for the excitation of the Zn^+ resonance lines appear in Fig. 4 and are presented in Table III. The behavior of the threshold is consistent with an infinitely steep rise folded with the 0.6-eV energy spread of the electron beam. In the energy region threshold to near 20 eV considerable structure is in evidence, and at higher energies the cross section falls off smoothly. The data below threshold are zero within the statistical precision, as expected, indicating that the measurements are free from a number of systematic effects.[7]

Data near threshold are presented in Fig. 5 on an expanded scale. It is probable that some of the observed structure above 11 eV is due to cascade. For example, the sudden increase at 12.2 eV is probably due to the onset of excitation of the $3d^{10}4d\,^2D$ term which decays by cascade through the $4p\,^2P$ term (Fig. 1). It is noted for reference that the emission lines $4\,^2D \rightarrow 4\,^2P$ are not resolved from the $4\,^2P \rightarrow 4\,^2S$ resonance lines in our apparatus. Thus, this cascade event is detected with nearly twice the probability of detecting a direct excitation event due to the fact that two photons result from the former. Other structures in the cross section do not correlate unambiguously with possible cascading levels. However, the minimum located at 9.8 eV between the $3d^9 4s^2\,^2D$ and $3d^{10}5s\,^2S$ terms lies in a region where there are no eigenstates of Zn^+, implying that this structure is due to resonance(s) with autoionizing states of neutral Zn (such resonances have been predicted[14] and observed[6,13,15] for many other scattering systems).

Also shown in Figs. 4 and 5 are three curves. One (dots) is calculated from the effective Gaunt factor, or $\bar{g}$-predictor formula[16–18] using the value for the optical oscillator strength[19] $f = 0.732$ chosen on the basis of a critical comparison[20] of experimental and theoretical data. The other curves are from a theoretical calculation by Msezane and Henry[12] using a five-state close-coupling (5CC) expansion. The 5CC results are presented both for $4s-4p$ excitation only (dashed, diamonds) and for a $4p$ emission cross section (solid, triangles) modeled as $\sigma(4p)=\sigma(4s,4p)+\sigma(4s,5s)+2\sigma(4s,4d)$, with the factor of 2 included for the reasons discussed above. We see that when allowance is made for cascade, the agreement with 5CC theory near threshold is excellent. The enhancement of the $4p$ cross section by cascade from $5s$ and $4d$ apparently is unusually large, being a factor of 1.64 at 15 eV and decreasing with increasing energy. Agreement with the $\bar{g}$-formula is excellent below the cascade thresholds, but worsens at higher energies due to cascade (the $\bar{g}$-formula results are for $4s-4p$ excitation only). Indeed, this strikingly good agreement near threshold is remarkable, in light of the factor of 2 uncertainty generally observed for this formula.[17,21]

The results at higher energies are best studied using the Bethe plot, or $\sigma \cdot E$ versus the logarithm

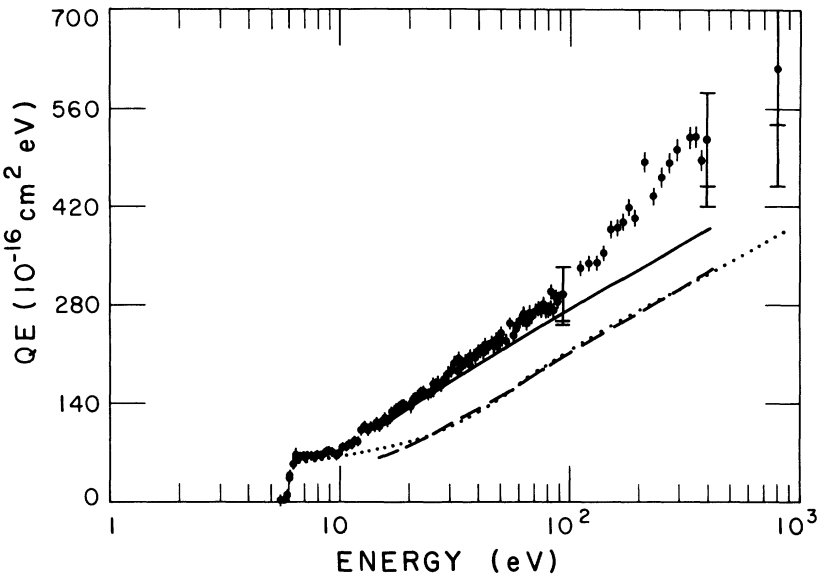

FIG. 6. Bethe plot for reaction in Eq. (1), showing σE vs log (E). $\bar{g}$ predictor formula results, · · · ; 5CC results (Ref. 12) without cascade contributions, — — —; 5CC results (Ref. 12) with cascade included (see text), —; present results, ●. Flags represent 68% CL absolute total uncertainty, with additional one-sided bars indicating possible effect due to uncollected electrons (see text and Tables I and II).

of E, the energy, shown in Fig. 6. In this figure the data are shown with a few representative [68% (CL)] error bars indicating absolute total uncertainty, with one-sided bars at energies greater than 100 eV indicating maximum possible effects of secondary electrons as described above. The data from about 20 to 100 eV fall on a fairly straight line, but near 100 eV the slope of the data increases to a value larger than the Bethe slope noted on the figure. Though the conservative estimates of the one-sided error due to secondaries is nearly large enough to account for the increased slope, it is interesting to note that such departures from the asymptotically accurate slope have been previously observed,[22] and that many excitation and ionization cross sections appear to have such a "pseudo-Bethe" regime in which the slope exceeds the Bethe slope. Above this region the cross sections tend to merge with the Bethe slope. Furthermore, there is evidence in other cases[3,13,23] that experimental cross sections have not yet reached the Bethe regime at energies as high as 120 threshold units.

Also shown in Fig. 6 are several calculations. The agreement between experiment and 5CC theory with cascade is excellent from 15 eV to approximately 100 eV, where the experimental slope changes. Also note the excellent agreement above 25 eV between 5CC without cascade and the $\bar{g}$-formula, both of which exhibit the "Bethe slope" above about 75 eV.

B. Zn^+ $4s-5s$ excitation results

The results of the measurement of the emission cross section for excitation of the $5s\ ^2S_{1/2}$ term of Zn^+ are given in Fig. 7 as well as in Table IV.

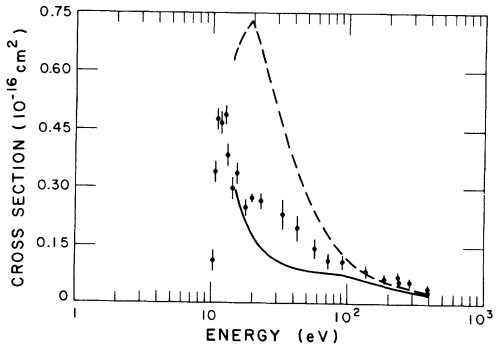

FIG. 7. Line-emission cross section for $5s$ excitation [Eq. (2)]. 2CC calculations (Ref. 12), — — —; 5CC calculations (Ref. 12), —; present results, ●. Flags indicate 68% CL relative uncertainties (Table I).

TABLE IV. Absolute emission cross sections for the process of Eq. (2): $e + Zn^+(4s\,^2S_{1/2}) \rightarrow e + Zn^+(nl\,^2L) \rightarrow h\nu(250.2, 255.8\ nm)$. Numbers in parentheses[a] represent percentage total *relative* uncertainty at 68% CL. Absolute uncertainties are given in Table II.

E (eV)	σ (10^{-17} cm^2)	E (eV)	σ (10^{-17} cm^2)
10.96	4.76(6)	42.65	1.96(7)
11.72	4.67(6)	57.60	1.44(8)
12.62	4.88(5)	72.40	1.12(9)
13.03	3.83(8)	92.27	1.09(9)
14.22	2.98(9)	137	0.85(9,11)
15.36	3.37(8)	186	0.66(10,12)
17.80	2.49(8)	236	0.71(10,13)
19.80	2.73(4)	239	0.58(9,12)
23.03	2.65(8)	285	0.56(12,16)
33.29	2.31(8)	388	0.35(11,17)

[a]Single numbers in parentheses indicate a uniform uncertainty, i.e., $(x) \equiv \pm x\%$. Two numbers in parentheses indicate the inclusion of one-sided uncertainties, i.e., $(x,y) \equiv +x\%, -y\%$.

Again, the threshold behavior is consistent with a finite threshold cross section folded with the energy distribution of the electron beam. The peak of the cross section, which occurs at threshold, is approximately $\frac{1}{20}$ of the resonance-line threshold cross section. There is some evidence for structure below the ionization limit of Zn^+, but the quantity and quality of the data are not sufficient to draw firm conclusions as to the origin of such structures. Below threshold the cross section is zero, again indicating absence of several possible systematic effects.[7] The results of the 2CC and 5CC calculations of Msezane and Henry[12] are included. Msezane and Henry state that their calculations are not converged due to the fact that other levels lying close to 5s are excluded from the close-coupling expansion. The data include cascading, which is not included in their calculations. No other calculations or measurements were found with which to compare the experimental data.

ACKNOWLEDGMENTS

We are grateful for many helpful discussions with Dr. R. J. W. Henry, and for the use of his and Dr. A. Z. Msezane's results prior to publication. This work was supported in part by the Office of Magnetic Fusion Energy, U. S. Department of Energy.

*Present address: National Bureau of Standards, Washington, D. C. 20234.
†Staff Member, Quantum Physics Division, National Bureau of Standards.
‡Permanent address: Laboratorio Metod. Av. Inorganiche, CNR, Rome, Italy.

[1]M. J. Seaton, *Advances in Atomic and Molecular Physics*, edited by D. R. Bates and B. Bederson (Academic, New York, 1975), Vol. 4, p. 83.
[2]I. C. Percival and M. J. Seaton, Philos. Trans. R. Soc. London Ser. A 251, 113 (1958).
[3]P. O. Taylor and G. H. Dunn, Phys. Rev. A 8, 2304 (1973).
[4]P. O. Taylor, Ph.D. thesis, University of Colorado, 1972, available through University Microfilms, Inc., Ann Arbor, Michigan (unpublished).
[5]P. O. Taylor, K. T. Dolder, W. E. Kauppila, and G. H. Dunn, Rev. Sci. Instrum. 45, 538 (1974).
[6]W. T. Rogers, J. Ø. Olsen, and G. H. Dunn, Phys. Rev. A 18, 1353 (1978).
[7]W. T. Rogers, Ph.D. thesis, University of Colorado, 1980, available through University Microfilms, Inc., Ann Arbor, Michigan (unpublished).
[8]M. Menzinger and L. Wahlin, Rev. Sci. Instrum. 45, 538 (1974).
[9]Exponential decay of the 589.6-nm photons resulting from decay of the $3d^9 4s^2\,^2D_{3/2}$ state was measured, giving an *effective* lifetime of 15.3 $(^{+3.8}_{-2.7})$ μsec. How-

ever, it was also determined from auxiliary ionization experiments that this lifetime includes cascade effects from high-lying levels, with evidence implicating either the $3d^9 4s\ ^1D\ 4p\ ^2P$ or $3d^9 4s\ ^1D\ 4p\ ^2D$ levels. Measurements which should be relatively free of cascade effects have been performed by Shearer and Holton [Phys. Rev. Lett. 24, 1214 (1970)] and by Osherovich *et al.* [Opt. Spectrosc. 46, 617 (1979)] to give 1.6 and 1.9 μsec, respectively, for the lifetime of the $3d^9 4s^2\ ^2D_{3/2}$ state.

[10]In the case of $e + Ca^+$ and Ba^+ the measured line-emission cross sections were in the ratios of the statistical weights at all energies [see Refs. 3 and 13].

[11]D. F. Dance, M. F. A. Harrison, and A. C. H. Smith, Proc. R. Soc. London Ser. A 290, 74 (1966).

[12]A. Z. Msezane and R. J. W. Henry, Phys. Rev. A 25, 692 (1982).

[13]D. H. Crandall, P. O. Taylor, and G. H. Dunn, Phys. Rev. A 10, 141 (1974).

[14]W. Fano and J. H. Macek, Rev. Mod. Phys. 45, 553 (1973).

[15]G. J. Schulz, Rev. Mod. Phys. 45, 378 (1973).

[16]A. Burgess, Mem. Soc. R. Sci. Liege 4, 299 (1961).

[17]M. J. Seaton, in *Atomic and Molecular Processes,* edited by D. R. Bates (Academic, New York, 1962), p. 374.

[18]H. Van Regermorter, Astrophys. J. 136, 906 (1962).

[19]C. Froese-Fischer, J. Phys. B 10, 1241 (1977).

[20]S. M. Younger and W. L. Wiese, Phys. Rev. A 18, 2366 (1978).

[21]G. H. Dunn, in *The Physics of Ionized Gases,* edited by M. Matić (Boris Kidrić Institute of Nuclear Sciences, Belgrade, 1980), p. 49.

[22]K. T. Dolder and B. Peart, Rep. Prog. Phys. 39, 693 (1976).

[23]E. A. Enemark and A. Gallagher, Phys. Rev. A 6, 192 (1972).